Malaria parasite *Plasmodium gallinaceum* up-regulates host red blood cell channels

Serge L.Y. Thomas[a,*], Stéphane Egée[a], Franck Lapaix[a], Lars Kaestner[a], Henry M. Staines[b], J. Clive Ellory[b]

[a] *Centre National de la Recherche Scientifique, UPR 9042, Station Biologique, Place G. Teissier, P.O. Box 74, 29682 Roscoff Cedex, France*
[b] *University Laboratory of Physiology, Parks Road, Oxford OX1 3PT, UK*

Received 18 April 2001; revised 31 May 2001; accepted 31 May 2001

First published online 13 June 2001

Edited by Matti Saraste

Abstract The properties of the malaria parasite-induced permeability pathways in the host red blood cell have been a major area of interest particularly in the context of whether the pathways are host- or parasite-derived. In the present study, the whole-cell configuration of the patch-clamp technique has been used to show that, compared with normal cells, chicken red blood cells infected by *Plasmodium gallinaceum* exhibited a 5–40-fold larger membrane conductance, which could be further increased up to 100-fold by raising intracellular Ca^{2+} levels. The increased conductance was not due to pathways with novel electrophysiological properties. Rather, the parasite increased the activity of endogenous 24 pS stretch-activated non-selective cationic (NSC) and 62 pS calcium-activated NSC channels, and, in some cases, of endogenous 255 pS anionic channels. © 2001 Published by Elsevier Science B.V. on behalf of the Federation of European Biochemical Societies.

Key words: Erythrocyte; Malaria; Ionic channel; Permeation pathway; *Plasmodium gallinaceum*

1. Introduction

Malaria-infected red blood cells (RBCs) possess parasite-induced transport pathways, which increase the uptake of selected nutrients and loss of metabolic waste products [1,2]. These pathways are obvious anti-malarial targets for selective inhibition [3], and routes for drug delivery [4], and it is therefore important to characterise these systems in some detail.

New permeation pathways (NPP) exist in human [5] and murine malaria-infected RBCs [6] and a reanalysis of earlier work [7] suggests their presence in malaria-infected avian RBCs. Kirk and co-workers [5] reported that the NPP in malaria-infected human RBCs are broad-specificity pathways of a single type, which show the characteristics of an anion channel. This has recently been supported by data from an electrophysiological investigation of infected human RBCs [8].

Electrophysiological studies represent the preferred method of choice for characterising the rapid transport of ions and charged organic solutes across membranes, but there have been few whole-cell patch-clamp studies on mammalian RBCs due to the fragility and small size of RBCs [8,9]. Since nucleated RBCs are more amenable to whole-cell patch-clamp studies and are amongst the earliest and easiest cells to be patched successfully [10,11], we have measured the membrane conductance of chicken RBCs infected by *Plasmodium gallinaceum*.

2. Materials and methods

2.1. Preparation of cells and malaria culture

Chicks (1–5 days old) were injected intravenously with 0.01 ml of chicken blood containing the malarial parasite *P. gallinaceum*, strain 8A, at approximately 20% parasitaemia. Parasitaemia, measured from Giemsa-stained blood smears, was in the range 50–75% 4 days after infection. At this point, the chicks were anaesthetised (intravenous Sagital injection) and blood samples (0.1 ml) were obtained from a wing vein. After sampling the animals were killed by intravenous overdose of Sagital. Blood was collected into NaCl saline containing (in mM) 150 NaCl, 5 KCl, 1.4 $CaCl_2$, 1 $MgCl_2$, 10 HEPES, 5 glucose, pH 7.4 and washed three times before use.

For patch-clamp experiments, infection by *P. gallinaceum* was visually assessed by modulation-contrast microscopy at 400×. Using this technique it was possible to distinguish between uninfected and infected RBCs in the unsynchronised cultures. However, it was not possible to resolve the developmental stage of the internal parasite.

2.2. Current recordings

Patch pipettes (tip resistance 4–10 MΩ) were prepared from borosilicate glass capillaries pulled and polished on a programmable puller. The whole-cell patch pipettes were filled with an intracellular-like K^+ solution ('Kint') containing (in mM): 145 KCl, 1 $MgCl_2$, 5 EGTA, 10 HEPES, 10 glucose, pH 7.2. This was also used as the bathing solution for excised patches. The patch pipettes used in cell-attached and excised inside-out configurations contained NaCl saline solution. Where appropriate the calcium concentration used in the bathing and the pipette solutions (pCa ($-\log[Ca^{2+}]$)) was adjusted between 8 and 3. All solutions were equilibrated in air and filtered through 0.2 μm Millipore cellulose discs.

Single-channel current and voltage recordings were made as described previously [12]. Increased membrane capacitance and reduction of the access resistance was used to assess the whole-cell configuration. Whole-cell current–voltage (I–V) relationships were run and analysed using WCP V3.2 software. Seal resistance was typically 4.0–6.0 GΩ and the series resistance (R_s) was typically 10–15 MΩ. Data are given as mean values ± S.E.M. Significance ($P < 0.001$) was assessed using Fisher's F-tests or Student's t-tests.

3. Results and discussion

3.1. Whole-cell patch-clamp of uninfected chicken RBCs

Using the whole-cell patch-clamp method, uninfected chicken RBCs showed low resting currents, which displayed linear I–V relationships (bath NaCl, pipette KCl media) with reversal potentials (E_r) close to 0 mV (Fig. 1a,c). The membrane

*Corresponding author. Fax: (33)-298-29 23 10.
E-mail: thomas@sb-roscoff.fr

0014-5793/01/$20.00 © 2001 Published by Elsevier Science B.V. on behalf of the Federation of European Biochemical Societies.
PII: S0014-5793(01)02579-0

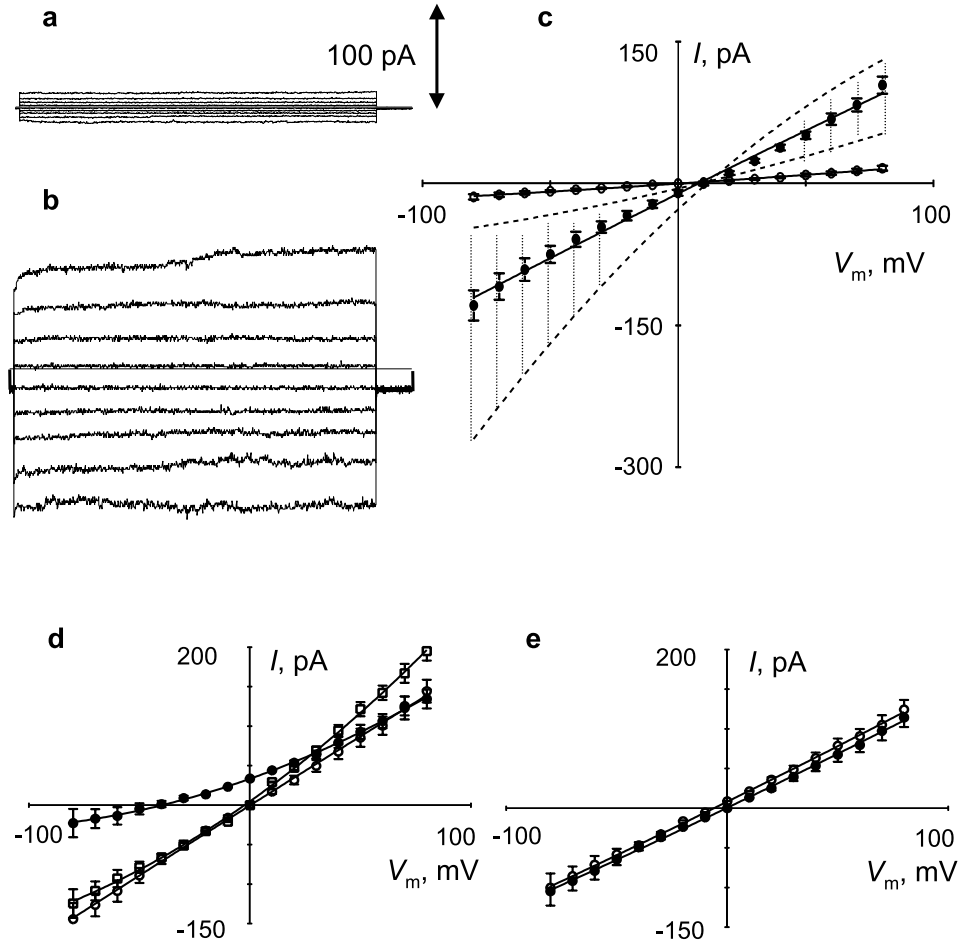

Fig. 1. Whole-cell recordings. Current traces in uninfected (a) or infected (b) RBCs, bathing in NaCl saline solution (voltage pulses between −80 and +80 mV, 20 mV increments, 400 ms). c: Corresponding *I–V* plots (mean ± S.E.M., 10 mV increments) from six uninfected (○) or 25 infected (●) cells. Dashed lines represent upper and lower limits of recorded current in infected cells. d: Mean *I–V* plots in infected cells, in control (○, $n=6$), and after replacement of cations by NMDG (●, $n=6$) or by choline (□, $n=5$) in the bathing solution. e: Replacement of Na^+ (○, $n=6$) by K^+ (●, $n=6$).

conductance (G_m) calculated near E_r was 178 ± 3 pS ($n=15$). Replacement of bath Na^+ by K^+ did not modify the membrane conductance significantly, but replacement by the impermeable cation *N*-methyl-D-glucamine (NMDG) almost totally abolished inward current. In addition, replacement of external chloride by the impermeable anion gluconate had no significant effect on the membrane conductance ($G_m = 168 \pm 8$ pS, $n=4$, near E_r). Given the transmembrane ionic gradients, these observations indicate that the membrane current of chicken RBCs is very low and is generated by non-selective cationic (NSC) channels.

3.2. Whole-cell patch-clamp of infected chicken RBCs

In marked contrast to the low membrane currents observed in uninfected chicken RBCs, the currents measured in infected RBCs were large (Fig. 1b,c) and variable. As the malaria cultures were unsynchronised, the large variability of the observed currents in infected RBCs may be attributable to the patching of infected RBCs at different stages of maturation. This would be consistent with previous reports of the stage-dependent activation of malaria-induced pathways [13,14].

In 90% of infected cells the current was 5–20-fold larger than in uninfected cells. The membrane current reversed polarity at 10.1 ± 0.2 mV ($n=25$) and the G_m, calculated near E_r, was measured to be 975 ± 20 pS ($n=25$). By comparing the conductances calculated at E_r, in these cells, 89 ± 5% ($n=6$) of the total inward current was abolished when Na^+ was replaced by NMDG in the bathing solution and the E_r shifted to −35 ± 4 mV ($n=6$) (Fig. 1d). However, only 18 ± 4% ($n=5$) of this current was abolished when choline was substituted for Na^+ (Fig. 1d), which indicates a significant choline permeability. The choline substitution data also showed an apparent increase in outward current, although further experimentation would be required to confirm whether it was significant and, if so, deduce its mechanism. Replacement of Na^+ by K^+ (Fig. 1e) or by the monovalent cations Cs^+, Li^+ or Rb^+ (data not shown) did not modify the membrane conductance significantly. In addition, replacement of external chloride by gluconate inhibited the outward current by only 8 ± 5% ($n=4$). The data indicate that the primary channels responsible for membrane conductance in infected cells are, like those observed in normal (uninfected) chicken RBCs, NSC channels.

In support of the ion substitution data, gadolinium (20 μM), a well-known inhibitor of NSC and stretch-activated (SA) NSC channels [15], inhibited membrane current in infected RBCs by 91 ± 5% ($n=6$). Flufenamic acid (0.1 mM)

and quinine (1 mM), also known as potent blockers of NSC channels [16,17], inhibited membrane current in infected RBCs by 22 ± 8% ($n = 6$) and 15 ± 9% ($n = 8$), respectively. In contrast, 1 mM 4,4′-diisothiocyanostilbene-2,2′-disulphonic acid (DIDS), 1 mM furosemide, 0.1 mM 5-nitro-2-(3-phenylpropylamino)-benzoate (NPPB), 10 μM tamoxifen and 1 mM glibenclamide had no significant effect.

In 10% of infected cells the current was 20–40-fold larger than in uninfected cells. In fact, channels could be observed as single-channel transitions during whole-cell current recording, in addition to the previously described membrane conductance. Fig. 2a shows a typical example of these recordings and Fig. 2b shows the corresponding single-channel I–V curve ($n = 10$). The single-channel slope conductance, calculated near E_r, was 241 ± 11 pS ($n = 10$). This channel was still present when Na^+ was replaced by NMDG in the bathing solution. Furthermore, the anion channel blockers NPPB (Fig. 2c) and tamoxifen (Fig. 2d) at concentrations of 0.1 mM and 10 μM, respectively, inhibited the channel totally. The data are consistent with the single-channel transitions occurring via a large anionic channel.

Interestingly, Ba^{2+} (1 mM), which is considered a general inhibitor of cationic channels [18], induced a large outward membrane current within 10 min of addition to the bath (data not shown). This effect was also observed in uninfected cells, although to a lesser extent. One possible explanation for this result is that intracellular Ba^{2+} ions are activating divalent cation-sensitive channels. If this is so, it may also be true that Ca^{2+} is capable of activating them. To test this hypothesis the free intracellular Ca^{2+} concentration ($[Ca^{2+}]_i$) of infected and uninfected cells was increased by addition of the Ca^{2+} ionophore A23187 (10 μM) to the bathing solution, in the presence of a 1 mM extracellular Ca^{2+} concentration ($[Ca^{2+}]_o$). This had the effect of increasing the membrane current within 20 min in infected cells (Fig. 3a) but failed to induce any effect in uninfected cells (Fig. 3b).

Furthermore, in an effort to establish whether $[Ca^{2+}]_o$ modulated the membrane conductance of uninfected or infected RBCs, experiments were performed over a range of $[Ca^{2+}]_o$ from 1 to 5 mM. However, there was no effect on the membrane conductance in uninfected or infected RBCs. The fact that whilst external Ba^{2+} was capable of activating a large conductance in both infected and uninfected cells, external Ca^{2+} was not, is very interesting. A possible explanation could be the activation of divalent cation-sensitive channels in response to an increased $[Ba^{2+}]_i$. This could be caused by Ba^{2+} permeating the RBC membrane to a greater degree than Ca^{2+} and/or by Ba^{2+} accumulating in the cytosol due to lowered extrusion via the Ca^{2+} pump. Alternatively, it could be explained by the involvement of divalent cation-sensitive channels, which are far more sensitive to Ba^{2+} than Ca^{2+}.

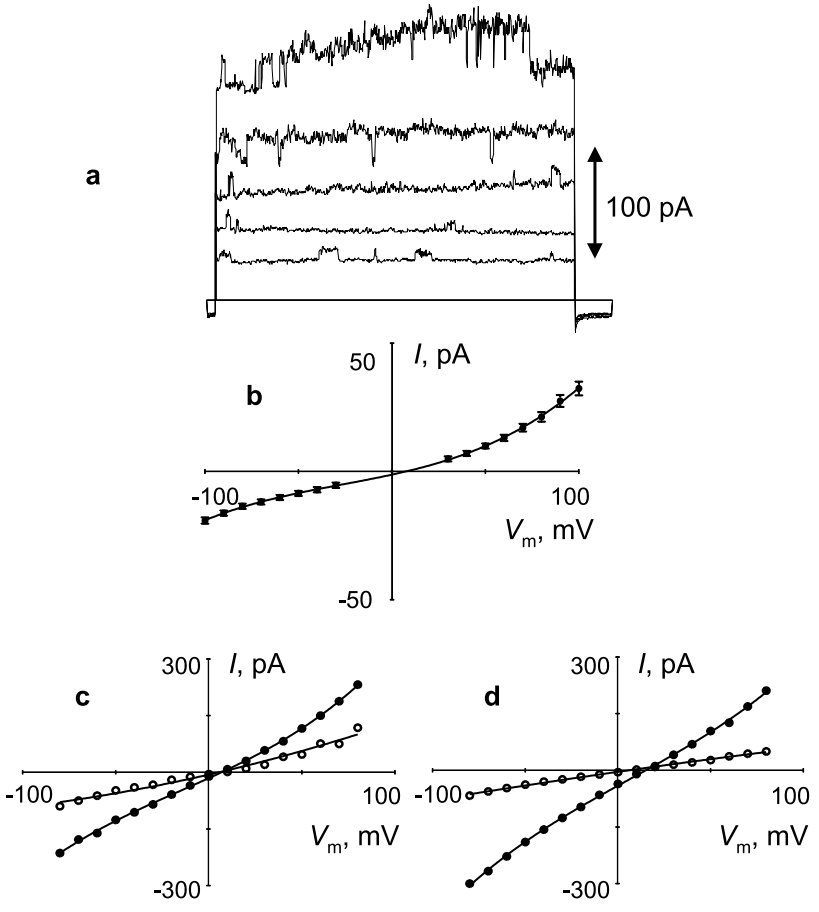

Fig. 2. Whole-cell recordings. a: Current traces in infected cells (voltage pulses between 0 and +100 mV, 20 mV increments, 400 ms) showing activation of large anionic channels. b: Mean single-channel I–V plot of activated anionic channels ($n = 10$). c: Typical example of whole-cell I–V plots from infected cells before (●) and after (○) addition of the anion channel blocker NPPB (0.1 mM). d: Typical example of whole-cell I–V plots from infected cells before (●) and after (○) addition of the anion channel blocker tamoxifen (10 μM).

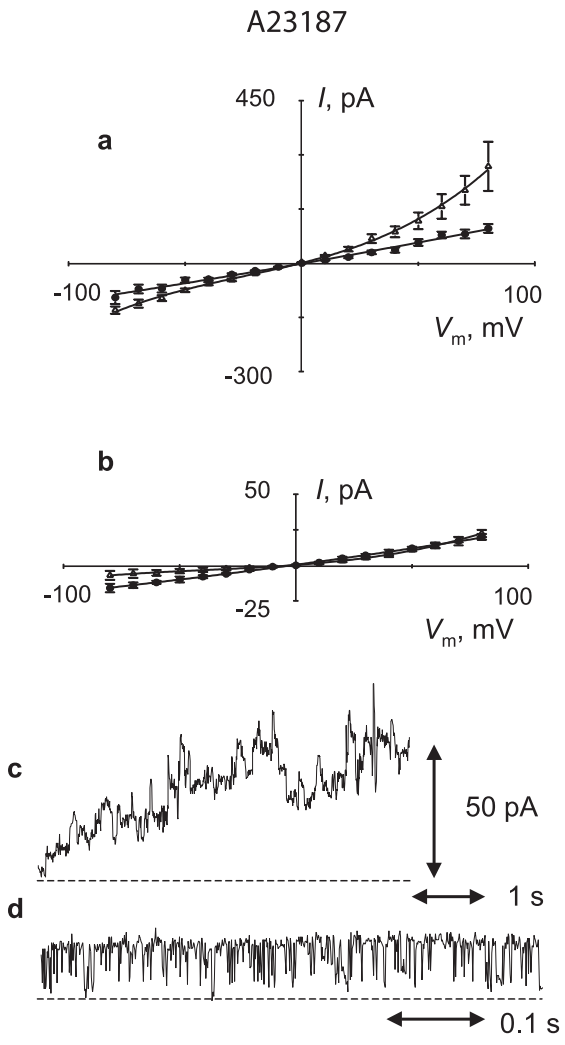

Fig. 3. Activation of membrane current by divalent cations. Mean *I–V* plots (±S.E.M.) obtained in infected cells (a, $n=6$) and uninfected cells (b, $n=6$), before (●) and 25 min after (△) addition of 10 μM A23187 in the bath. c: Single-channel transitions on whole-cell recordings, showing recruitment of eight new NSC channels (6 pA each) 5 min after addition of 10 μM A23187 in the bath (+80 mV). d: Presence of a large (20 pA) anionic channel 25 min after addition of 10 μM A23187 (+80 mV).

In infected cells, the recruitment of new channels was clearly visible after addition of the ionophore to the bathing solution (Fig. 3c) and could be inhibited by gadolinium (20 μM). These observations indicate the existence of Ca^{2+}-sensitive conductive pathways in infected cells, which could correspond either to an increased Ca^{2+} sensitivity of pre-existing pathways or to metabolic effects as a consequence of prolonged Ca^{2+} loading, which may explain the short lag phase observed before channel activation. These enhanced currents showed similar cation selectivity, and sensitivity to gadolinium, flufenamic acid and quinine as the untreated infected cells, implying that similar NSC channels are involved.

However, the anion channel inhibitors NPPB (0.1 mM) and tamoxifen (10 μM) blocked 18±5% ($n=8$) and 22±4% ($n=6$), respectively, of the induced current, suggesting the appearance of an anionic component in addition to the NSC channels. Fig. 3d shows the appearance of the NPPB-sensitive anionic channels in infected RBC in the presence of the ionophore.

3.3. Excised patch-clamp of uninfected and infected chicken RBCs

The excised inside-out configuration was used to identify directly the different channel types present in the plasma membranes of uninfected and infected chicken RBCs. The majority of successful patches ($n=127$, i.e. 80–85% of uninfected RBCs; $n=82$, i.e. 80–85% of infected RBCs) contained spontaneously active channels. The average seal duration was twice as long in uninfected RBCs, but the percentage of active patches was not different in infected compared with uninfected RBCs. The data presented in Fig. 4 were obtained using excised patches from uninfected cells. However, identical data were also obtained using excised patches from infected cells (i.e. no differences were found between uninfected and infected excised patches).

With NaCl saline in the bath and Kint (pCa 8) in the pipette, two channel types were measured, with linear *I–V* relationships. Unit conductances were 23.8±0.1 pS ($n=12$) and 62.4±1.2 pS ($n=15$) in uninfected patches (Fig. 4a), respectively, and the E_r was not different from 0 mV. Unit conductances in infected patches were 24.2±0.1 pS ($n=15$) and 65.0±2.7 pS ($n=12$), respectively. Substitution of K^+, Cs^+, Li^+ or Rb^+ for Na^+ in the pipette or in the bath did not significantly change the single channel conductances. Dilution of the bathing solution KCl concentration shifted the reversal potential towards the Nernst equilibrium for cations and replacement of K^+ or Na^+ with NMDG in the bath abolished the outward current. The data are consistent with the presence of two types of NSC channels.

The small conductance NSC channel was mechano-sensitive. Application of a negative pressure in the pipette induced the activation of channels in quiescent patches (Fig. 4b), or recruitment of new channels in active patches. Open probability (P_o), measured at a given membrane potential, was related to the degree of deformation imposed on the membrane patch. This SA-NSC channel was permeable to divalent cations with $P_{Ca}/P_{Na}=0.6$ and $P_{Ba}/P_{Na}=0.8$. Gadolinium (10 μM) applied in the pipette completely blocked the channel, quinine (1 mM) produced a partial reduction of P_o (20–40%, $n=5$) and flufenamic acid (100 μM) had no effect.

The large-conductance NSC channel exhibited three substates with full opening only displayed at membrane potentials above +60 mV or below −60 mV (Fig. 4c). It was not affected by the application of a negative pressure in the pipette (i.e. it is not stretch-activated), but was Ca^{2+}-sensitive. Channel activity was observed in the 10^{-7} M range of Ca^{2+} concentration with maximum activity at 10^{-5} M (Fig. 4d). This channel was permeable to choline ($K^+(1)=Na^+(1)>$choline(0.8)), and was inhibited by 100 μM flufenamic acid and 1 mM quinine added in the bath solution. Gadolinium (10 μM) applied in the pipette blocked only 15±8% ($n=5$) of channel activity, by progressive reduction of P_o.

Consistent with the occurrence of occasional single-channel openings, of large amplitude, observed in whole-cell recordings of infected cells, the presence of a large channel was observed in 5–10% of membrane patches in infected as well as in uninfected RBCs (Fig. 4e). This channel disappeared rapidly after excision but it was possible to reactivate the channel by subjecting the patch to a −120 mV pulse for a

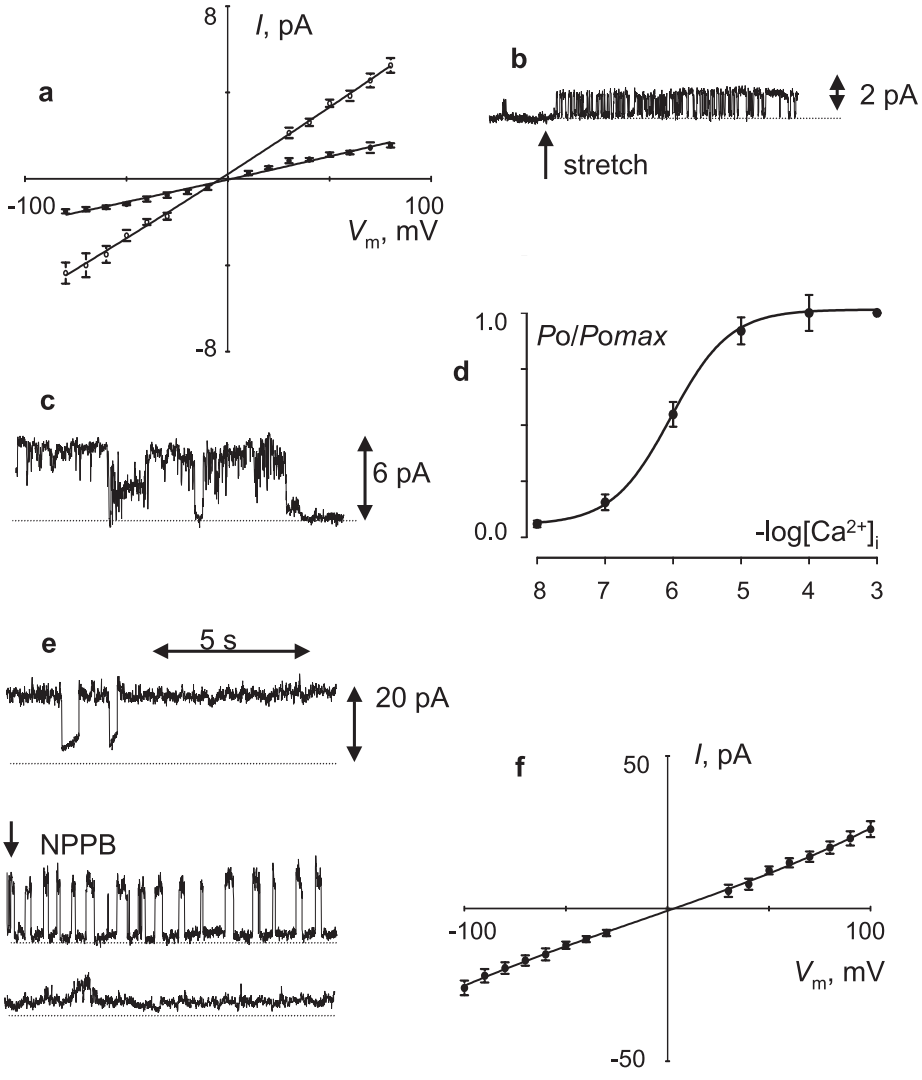

Fig. 4. Single-channel recordings in uninfected cells. a: Mean *I–V* plots (±S.E.M.) obtained in excised inside-out patches of small (●) ($n=12$) and large (○) ($n=15$) NSC channels (V_m, membrane potential, negative of pipette potential). b: Stretch activation of a small NSC channel (+80 mV, 10 mm Hg negative pressure). Dotted lines: closed state. c: Current recordings of a large NSC channel displaying multiple sub-states (+80 mV). d: Calcium activation of large NSC channels (pCa = −log [Ca^{2+}], +80 mV). e: Current recordings of a large chloride channel, inhibition by 100 μM NPPB. f: Corresponding *I–V* plot ($n=15$).

few seconds. This approach allowed this channel to be observed in 75–85% of infected and uninfected RBCs. The single channel *I–V* relationship was linear (Fig. 4f) with a slope conductance of 255 ± 8 pS ($n=15$) in uninfected patches and 248 ± 12 pS ($n=9$) in infected patches. This channel exhibited voltage-dependent gating, with negligible P_o between −40 mV and +40 mV. Replacement of K^+ by Na^+ or by NMDG had no significant effect upon the *I–V* relationship and NPPB (Fig. 4e) or tamoxifen at concentrations of 0.1 mM and 10 μM, respectively, inhibited channel activity completely. The data are consistent with the presence of an anion channel. The anionic nature of the channel was confirmed by changing from Kint to half-strength Kint, which reduced the KCl concentration on the cytosolic side of the patch by half. This had the effect of shifting significantly the *I–V* curve to the left, with a calculated reversal potential of −12.5 ± 2.2 mV ($n=6$). This is close to the Nernst equilibrium for Cl^- (−17.5 mV). Changing the Ca^{2+} concentration from 1 to 5 mM in the bathing solution had no effect on single-channel activity.

After excision, two types of NSC channels and a large anion channel were observed in most membrane patches with exactly the same frequency of occurrence in both uninfected and infected RBCs. Thus, the two situations (control and infected) were identical at the level of the excised patch.

3.4. Conclusions

The data presented here show an increase in the membrane conductance of avian RBCs after malaria infection. However, in marked contrast to recent results on malaria-infected human RBCs [8], we find no evidence of new conductive pathways in the infected cell. Rather, the parasite increases the activity of endogenous pathways present in the host membrane. This distinction is important because it represents the simplest strategy for modifying cell volume and ionic composition in the infected cell. It raises the possibility that the

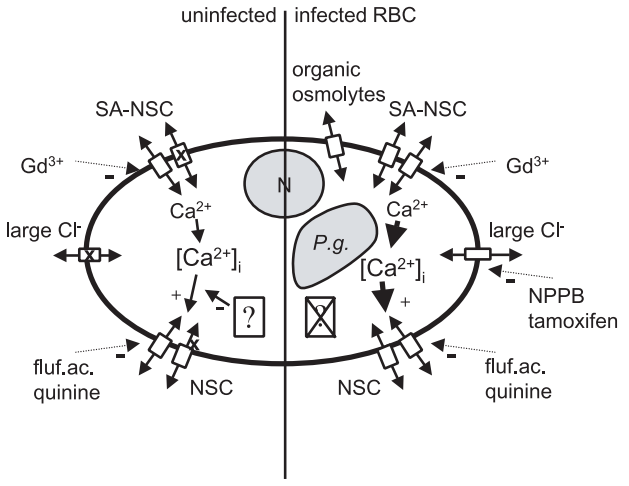

Fig. 5. Schematic diagram. Two types of NSC channel (stretch-activated 24 pS and 62 pS) and a large anion channel (255 pS) were observed with the same frequency of occurrence in excised patches from both uninfected and *P. gallinaceum*-infected (*P.g.*) RBCs. Activation of the SA-NSC leading to a gadolinium-inhibitable Ca^{2+} permeability would in turn activate the large Ca^{2+}-dependent NSC channels, which show increased calcium sensitivity (represented by thick solid arrows) in infected cells. This enhanced Ca^{2+} sensitivity may involve the removal of a cytosolic factor or effect (?), which suppresses the Ca^{2+} sensitivity of the large NSC channels in uninfected cells. The large-conductance anionic channels are active in infected cells and quiescent in uninfected cells. This diagram also shows the existence of novel channel(s) for electroneutral organic osmolyte transport in malaria-infected chicken RBCs. Nucleus (N).

small-conductance channels identified by Desai and co-workers [8], as novel malaria-dependent pathways, are also endogenous components of the human red cell membrane, and there are some indications in the literature [19,20] that this may be so. Furthermore, the role of divalent cations in promoting these effects suggests that intracellular Ca^{2+} may play a key role in this activation in the parasitised cell.

Combining the data presented in this paper to produce a summary diagram, Fig. 5 shows a schematic model of the type of conductive channels and their state of activation, in uninfected and malaria-infected avian RBCs. In uninfected cells there are three channel types present, two NSC channels and an anion channel. The observed low conductance in uninfected cells is due to the activity of a low number and/or P_o of the two NSC channels, while the anion channel is quiescent. The Ca^{2+} sensitivity of the larger NSC channel (observed in excised patches) in uninfected cells is suppressed, presumably by a cytosolic factor. In infected cells there are the same three channel types. The observed increase in conductance in infected cells is caused predominantly by the activity of an increased number and/or P_o of the two NSC channels. However, the anion channel can also be activated and increase the conductance in infected cells.

The identity of the proposed cytosolic factor that modifies the activity, or rather Ca^{2+} sensitivity, of the large-conductance NSC channel observed in chicken RBCs remains to be established. Obvious candidates would be kinases/phosphatases sensitive to Ca^{2+}, which would regulate channel activity. Alternatively, raised intracellular Ca^{2+} levels may deplete ATP levels via the Ca^{2+}-ATPase with subsequent effects on cellular metabolism, which would subsequently alter channel activity indirectly.

The reasons for the increase in conductance of the three channel types in infected cells are not known. The small SA-NSC channel could be activated directly by the parasite (e.g. phosphorylation) or activated indirectly by the growing parasite stretching the host cell membrane. The large NSC channel was shown to uncover a pre-existing Ca^{2+} sensitivity after parasite invasion and so $[Ca^{2+}]_i$ may be responsible for its increased activity. As for the anionic channel, one possible reason why it is activated may be to act as a 'shunt' pathway to preserve electroneutrality. However, the fact that this channel is rarely seen in the whole-cell configuration suggests its activation is complex and makes its physiological status uncertain.

One possible role for these conductance pathways is to aid volume regulation. The small NSC channel was shown to conduct Ca^{2+}, and Ca^{2+} permeation is a feature of SA-NSCs. It may act as the primary signal of cell swelling [21], allowing the influx of Ca^{2+}, which in turn activates the large Ca^{2+}-dependent NSC channels. This process would decrease the cell volume, as reported for other cell types [22]. In this case, the possible contribution of these two NSC channels to the permeation pathways in the parasitised cell depends on the magnitude of the change in $[Ca^{2+}]_i$ and of the increase in Ca^{2+} sensitivity of the large NSC channels.

An obvious question must be how similar the infected chicken RBC is to the human case. The characterised channels are summarised in Table 1. It can be concluded that there are general similarities with increased conductive pathways in both species of infection, but that channels responsible for the increased conductance are different in parasitised human cells compared with parasitised avian cells. Our main conclusion, that endogenous pathways are up-regulated in infected chicken RBCs rather than the introduction of new channels, is important and the opposite of published work on human cells

Table 1
A comparison of malaria-induced conductance pathways

	Conductive pathway			
	Human (*P. falciparum*) [8]	Chicken (*P. gallinaceum*)	Chicken (*P. gallinaceum*)	Chicken (*P. gallinaceum*)
Nature	Anion channel	NSC channel	NSC channel	Anion channel
Size	<10 pS	24 pS	62 pS	255 pS
Selectivity	$SCN^- > I^- > Br^- > Cl^- >$ acetate$^-$ > lactate$^-$ > glutamate$^-$	Na^+, K^+, Rb^+, Cs^+, $Li^+ > Ba^{2+} > Ca^{2+}$	Na^+, K^+, Rb^+, Cs^+, $Li^+ >$ choline$^+$	Cl^-
Inhibitors	NPPB > furosemide, glibenclamide, niflumate ≫ DIDS	Gadolinium ≫ quinine > flufenamic acid	Quinine, flufenamic acid ≫ gadolinium	NPPB, tamoxifen
Voltage sensitivity	Inward rectification	Linear	Linear	Linear (but inactive between +40 and −40 mV)
Activators	None reported	Stretch-activated	Ca^{2+}-sensitive	−120 mV pre-pulse

[8]. It is clearly essential to investigate the situation further in human cells, to resolve this important apparent contradiction.

Malaria-infected human and avian RBCs also show increased transport of a variety of non-electrolytes [5,7]. There is also good evidence for enhanced sorbitol and taurine uptake into malaria-infected chicken RBCs under physiological conditions via a malaria-induced pathway [23]. This suggests that, although the present electrophysiological studies rule out the parasite-related induction of new conductive pathways, novel channel(s) for electroneutral and organic osmolyte transport (measured in tracer flux studies) are induced in malaria-infected chicken RBCs (see Fig. 5). A fuller understanding of the physiological roles of the various channels active in infected cells may be important in developing strategies for future malarial chemotherapy.

Acknowledgements: We thank R. Paul and A. Raibaud, Institut Pasteur, Paris, for providing *P. gallinaceum* and for helpful discussions. This work was supported by the MENRT (PRFMMIP), the Wellcome Trust (Grant 058230) and the Fondation Langlois.

References

[1] Ginsburg, H. (1999) in: Transport and Trafficking in the Malaria-Infected Erythrocyte (Bock, G.R. and Cardew, G., Eds.), pp. 99–108, Novartis Found. Symp. 226, Wiley, Chichester.
[2] Kirk, K. (2000) Nature 406, 949–951.
[3] Macreadie, I., Ginsburg, H., Sirawaraporn, W. and Tilley, L. (2000) Parasitol. Today 16, 438–444.
[4] Kirk, K., Tilley, L. and Ginsburg, H. (1999) Parasitol. Today 15, 355–357.
[5] Kirk, K., Horner, H.A., Elford, B.C., Ellory, J.C. and Newbold, C.I. (1994) J. Biol. Chem. 269, 3339–3347.
[6] Staines, H.M. and Kirk, K. (1998) Biochem. J. 334, 525–530.
[7] Sherman, I.W. and Tanigoshi, L. (1974) J. Protozool. 21, 603–607.
[8] Desai, S.A., Bezrukov, S.M. and Zimmerberg, J. (2000) Nature 406, 1001–1005.
[9] Huber, S. M., Gamper, N. and Lang, F. (2000) Eur. J. Physiol. online.
[10] Hamill, O.P. (1983) in: Single Channel Recording (Sakmann, N. and Neher, E., Eds.), pp. 451–471, Plenum, New York.
[11] Egée, S., Harvey, B.J. and Thomas, S. (1997) J. Physiol. 504, 57–63.
[12] Egée, S., Lapaix, F., Cossins, A.R. and Thomas, S. (2000) Bioelectrochemistry 52, 133–149.
[13] Elford, B.C., Haynes, J.D., Chulay, J.D. and Wilson, R.J. (1985) Mol. Biochem. Parasitol. 16, 43–60.
[14] Staines, H.M., Chang, W., Ellory, J.C., Tiffert, T., Kirk, K. and Lew, V.L. (1999) J. Membr. Biol. 172, 13–24.
[15] Yang, X.C. and Sachs, F. (1989) Science 243, 1068–1071.
[16] Yeh, T., Van den Abbeele, T., Marianovski, R., Herman, P. and Tran Ba Huy, P. (1995) Hear. Res. 90, 79–88.
[17] Gogelein, H. and Capek, K. (1990) Biochim. Biophys. Acta 1027, 191–198.
[18] Lattore, R. and Miller, C. (1983) J. Membr. Biol. 71, 11–30.
[19] Schwartz, R.S., Rybicki, A. and Nagel, R.L. (1997) Biochem. J. 327, 609–616.
[20] Freedman, J.C., Novac, T.S., Bisognano, J.D. and Pratap, P.R. (1994) J. Gen. Physiol. 104, 961–983.
[21] Christensen, O. (1987) Nature 330, 66–68.
[22] Christensen, O. and Hoffmann, E.K. (1992) J. Membr. Biol. 129, 13–36.
[23] Staines, H.M., Godfrey, E.M., Lapaix, F., Egée, S., Thomas, S. and Ellory, J.C. (2001) Biochim. Biophys. Acta (submitted).